Supporting Information

Synthesis of stable γ-phase $MnS_{1-x}Se_x$ nanoflakes with inversion symmetry breaking

Bo Zheng[1#], Jun Fu[2#], Yuanmin Zhu[3,6#], Jing Liang[4#], Yongzhi She[5], Junxiang Xiang[1], Xiang Ma[1], Ying Zhang[1], Shasha Wang[1], Guojing Hu[1], Yuehui Zhou[1], Yan Feng[1], Zhengping Fu[1], Nan Pan[5], Yalin Lu[1]*, Hualing Zeng[2], Meng Gu[6], Kaihui Liu[4], Bin Xiang[1]*

Note S1: Similar to the reported work, the SHG intensity increase with the increase of incident laser power, showing a parabola-like shape ($I \propto P^{\theta}$, $\theta = 2.04 \pm 0.02$), because SHG is a second-order nonlinear optical process, which should be quadratic proportional to the incident laser intensity. The electric dipole theory forecasts that under the first-order perturbation $I_{SHG} = |E(2\omega)|^2 \propto |P(\omega)|^2$, where I_{SHG} is the SHG intensity, $E(2\omega)$ is SHG electric field vector, and $P(\omega)$ is excitation power[1].

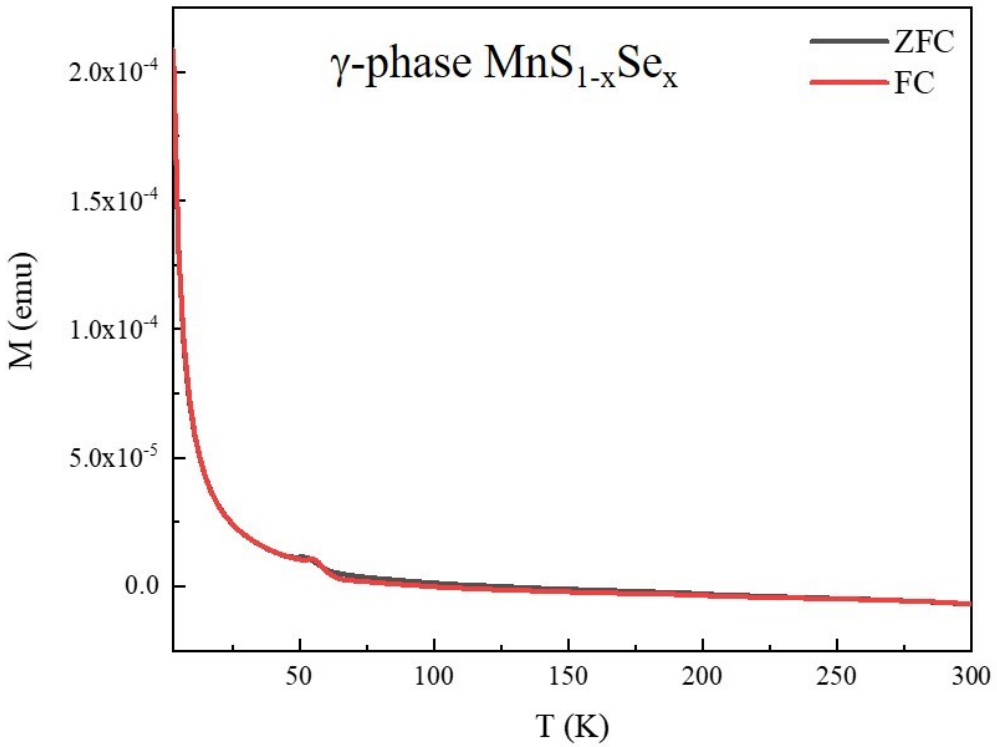

Figure S1. ZFC and FC magnetization curves of γ-phase $MnS_{1-x}Se_x$ (x=0.09) nanoflakes measured with the external magnetic field H = 9 T applied along the c axis.

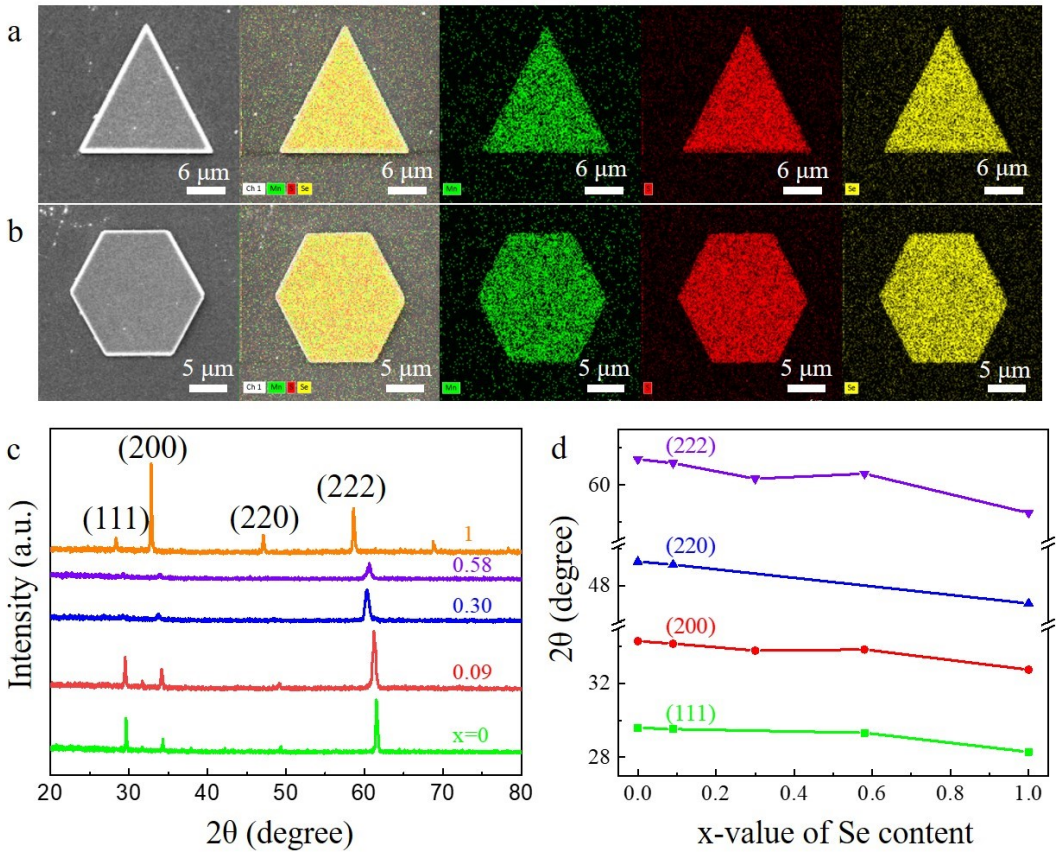

Figure S2. EDS elemental mapping images of Mn, S and Se in a typical $MnS_{1-x}Se_x$ (x=0.30) nanosheet with the shape of a triangle (a) and hexagon (b). (c) XRD patterns of as-synthesized α-phase $MnS_{1-x}Se_x$ nanosheets with x values of 0, 0.09, 0.3, 0.58 and 1. (d) Plots of XRD diffraction peaks determined from (c) as a function of the Se composition x.

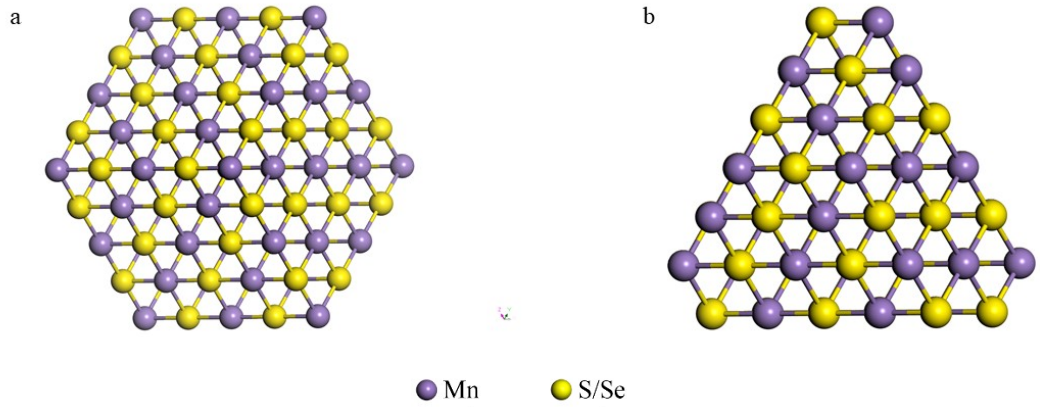

Figure S3. The ball-and-stick models of the α-phase $MnS_{1-x}Se_x$ crystal with the shape of hexagon (a) and triangle (b).

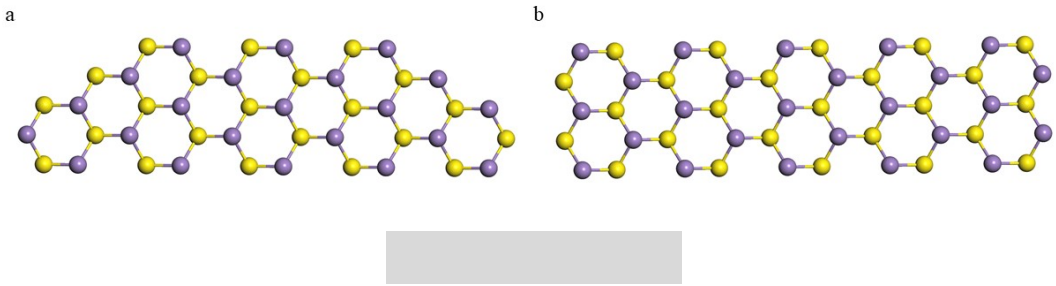

Figure S4. The ball-and-stick models of the γ-phase $MnS_{1-x}Se_x$ crystal with the shape of trapezoid (a) and rectangle (b).

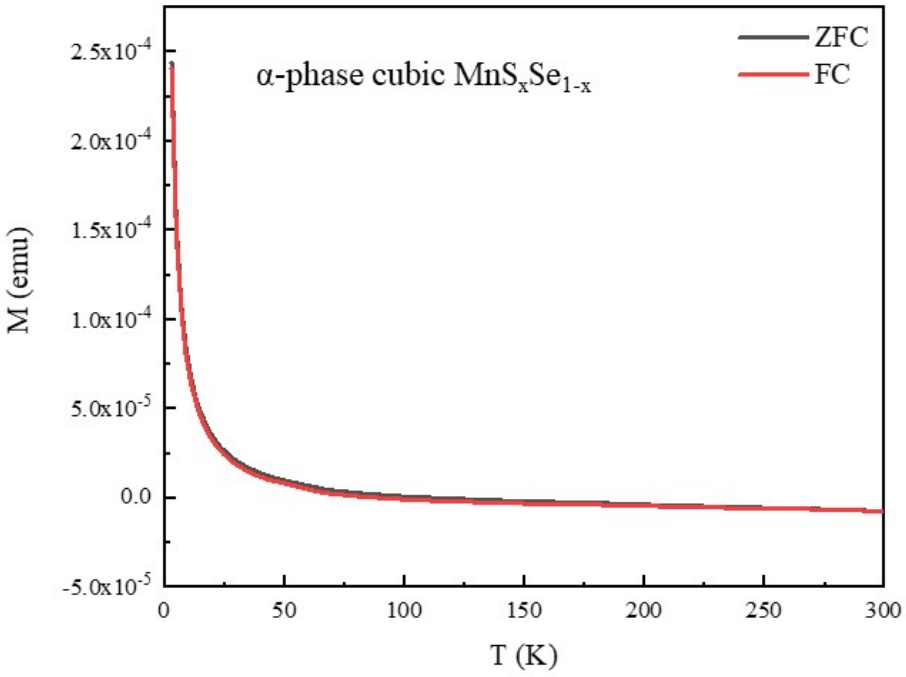

Figure S5. ZFC and FC magnetization curves of α-phase $MnS_{1-x}Se_x$ (x=0.58) measured with the external magnetic field H = 9 T applied along the c axis.

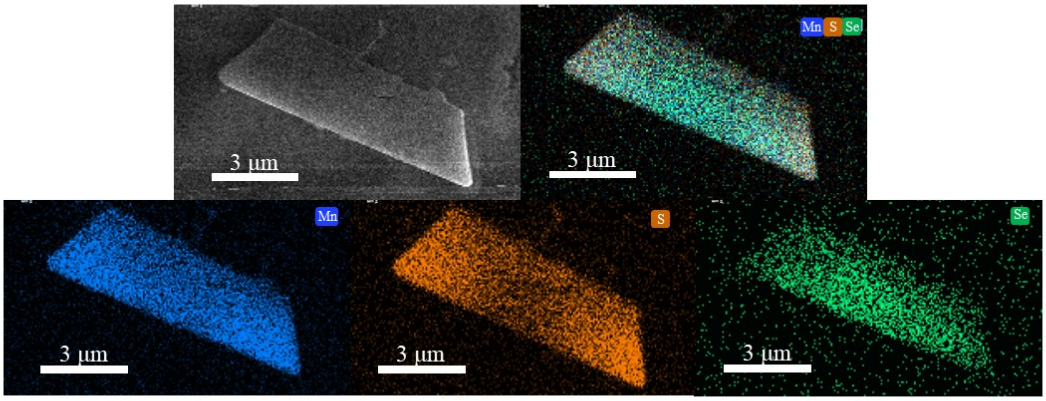

Figure S6. EDS elemental mapping images of Mn, S and Se in a typical γ-phase $MnS_{1-x}Se_x$ (x=0.27) nanosheet with the shape of a trapezoid.

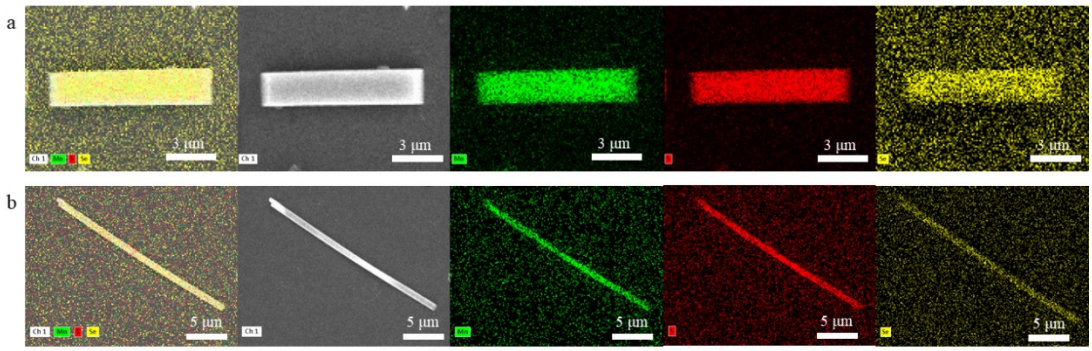

Figure S7. EDS elemental mapping images of Mn, S and Se in a typical rectangular (a) γ-phase $MnS_{1-x}Se_x$ (x=0.09) nanosheet and (b) γ-phase $MnS_{1-x}Se_x$ (x=0.27) nanowire.

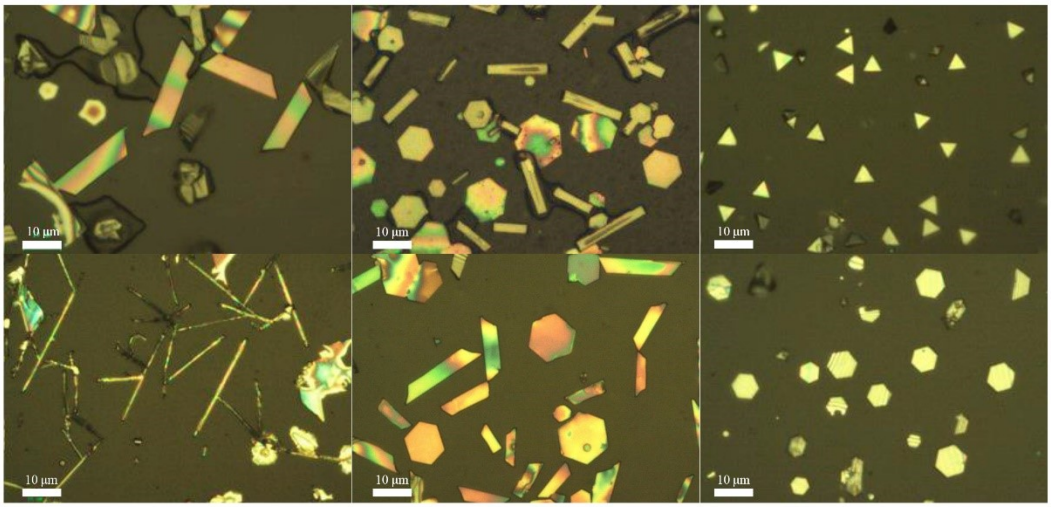

Figure S8. The different morphology of γ-phase $MnS_{1-x}Se_x$ (x=0.09) and α-phase $MnS_{1-x}Se_x$ (x=0.30).

	x value (calculated from precursor loading amount)	x value of γ-$MnS_{1-x}Se_x$ (obtained from EDS)	x value of α-$MnS_{1-x}Se_x$ (obtained from EDS)
1	0	0	0
2	0.25	0.02	0.09
3	0.5	0.09	0.30
4	0.75	0.27	0.58
5	1	0.45	1

Table S1. The x value of the as-grown γ-phase $MnS_{1-x}Se_x$ and α-phase $MnS_{1-x}Se_x$.

REFERENCES

1. X. Zhou, J. Cheng, Y. Zhou, T. Cao, H. Hong, Z. Liao, S. Wu, H. Peng, K. Liu and D. Yu, *J. Am. Chem. Soc.*, 2015, **137**, 7994-7997.